THE ASTRONOMICAL JOURNAL, 115:2509–2514, 1998 June

H_2O ICE IN THE ENVELOPES OF OH/IR STARS

A. W. MEYER,[1] R. G. SMITH,[2] S. B. CHARNLEY,[3] AND Y. J. PENDLETON
Space Science Division, MS 245-3, NASA Ames Research Center, Moffett Field, CA 94035
Received 1997 November 12; revised 1998 February 17

ABSTRACT

In an attempt to better understand the conditions under which molecules condense onto grains in the envelopes of evolved stars, we have searched for the presence of H_2O ice in the circumstellar envelopes of several evolved (OH/IR) stars. The sample of stars observed was selected on the basis of mass-loss rates, luminosities, and outflow velocities in order to cover a range of physical conditions that might affect the amount of ice present in stellar envelopes. Despite the clear presence of H_2O ice around other, previously observed, evolved stars, our search in six OH/IR stars has resulted in only one clear detection, in OH 26.5+0.6, and the tentative detection in one other, OH 26.4−1.9. We provide column densities or upper limits for the amount of ice that is present on the grains around these stars and explore the possibility that there could be a relationship between $\dot{M}_*$ or $\dot{M}_*/L_*$ and the H_2O ice column density to explain the observations.

Key words: dust, extinction — infrared radiation — ISM: clouds — stars: late-type

1. INTRODUCTION

Substantial mass outflow leading to a circumstellar envelope or shell is a common, although not necessarily well understood, feature of evolved stars. Several authors have tried to model the condensation in these envelopes—Jura & Morris (1985) used analytic methods to model the condensation onto grains in the outflows from mass-losing red giants, whereas Charnley & Smith (1993) used a numerical model to treat both the gas-grain interactions and the molecular chemistry that take place as outflowing material moves through the envelope. However, from this and other work it has become clear that successful modeling of these envelopes requires a much better understanding of the physics and chemistry of the envelopes, particularly in the case of gas-grain interaction. By performing a systematic study of the dust and gas around these stars, we can constrain the physical conditions and molecular abundances in the outflows and so improve stellar evolutionary models.

To this end, we have begun a systematic study of the dust in a subset of evolved stars, the dust-enshrouded asymptotic giant branch (AGB) or OH/IR stars. Evolution on the final part of the AGB is accompanied by substantial mass loss, often leading to thick dust envelopes. The standard evolutionary scenario for the envelopes is that some form of silicate grains nucleate in the hot material flowing out from the star, somewhere around 5–10 stellar radii (R_*), at temperatures around 1000 K. The grains are then driven outward by radiation pressure, dragging the gas along with them (e.g., Tielens 1983). Of the few observable spectral characteristics of circumstellar dust grains, the silicate features near 9.7 and 18 μm are the most prominent. In the cooler regions of the envelope, gas-phase molecules can condense onto the grains. One molecule that must condense far out in the envelope is H_2O, as a consequence of its low condensation temperature ($\lesssim$110 K; Nakagawa 1980). Of course, whether significant amounts of ice condense at all depends strongly on the radial distribution of density and temperature (e.g., Charnley & Smith 1993), as well as other properties of the star and dust envelope.

The spectra of several evolved stars do in fact show broad absorption features in the infrared near 3.1 μm that can be attributed to H_2O ice in or on the grains in a circumstellar envelope or disk. These stars are OH 231.8+4.2 (also known as OH 0739−14; Gillett & Soifer 1976; Smith, Sellgren, & Tokunaga 1988), OH 32.8−0.2 (Roche & Aitken 1984), IRAS 09371+1212 (Rouan et al. 1988; Hodapp, Sellgren, & Nagata 1988; Geballe et al. 1988), OH 344.1+5.8 (also known as IRAS 16342−3814; van der Veen 1988), and M1-92 (Eiroa, Hefele, & Qian 1983). However, given five examples, we may then ask how common the phenomenon of H_2O ice condensation on grains in circumstellar envelopes is and what particular physical conditions in the envelopes of these stars have led to this condensation. In an attempt to answer these questions, and also to look at one aspect of the gas-grain interaction in circumstellar outflows that might provide the basis for improved models of condensation in circumstellar envelopes, we have obtained 2.0–3.8 μm moderate-resolution infrared spectra of a sample of OH/IR stars to search for evidence of the broad absorption feature of H_2O ice near 3.1 μm.

The sample of stars observed was selected on the basis of mass-loss rates, outflow velocities, and luminosities, covering a range of physical conditions that might conceivably affect the amount of ice present in the stellar envelopes. In selecting the sample, we drew upon the work of Herman & Habing (1985), van der Veen (1989), Werner et al. (1980), Sopka et al. (1985), and Jones, Hyland, & Gatley (1983). We were also guided in the source selection process by the work of Jura & Morris (1985), who modeled the condensation onto grains in the outflows from mass-losing red giants (Jura & Morris applied their results, for example, to OH 231.8+4.2, OH 32.8−0.3, and OH 26.5−0.6). Our choice of objects was further restricted, however, by the requirement

[1] Visiting Astronomer, Cerro Tololo Inter-American Observatory, National Optical Astronomy Observatories, operated by the Association of Universities for Research in Astronomy, Inc., under cooperative agreement with the National Science Foundation.

[2] Permanent address: School of Physics, University College, University of New South Wales, Australian Defence Force Academy, Canberra, ACT 2600, Australia.

[3] Also Department of Astronomy, University of California, Berkeley.

TABLE 1

LOG OF OBSERVATIONS

Source	Date (1995)	Air Mass	Range (μm)	t_{int} (s)	Standard Star	Spectral Type	Blackbody Temperature (K)
OH 12.8−1.9.....	July 6	1.30	2.15–2.32	40	HR 6378	A2 V	9100
	July 6	1.25	2.27–2.44	18			
	July 6	1.19	2.88–3.22	6.3			
	July 6	1.12	3.16–3.50	4.5			
	July 6	1.11	3.44–3.78	3.6			
OH 20.3−0.1.....	July 6	1.25	2.15–2.32	120	HR 7236	B9 V	21000
	July 6	1.28	2.27–2.44	120			
	July 6	1.54	2.88–3.22	9			
	July 6	1.61	3.16–3.50	5.4			
	July 6	1.85	3.44–3.78	3.6			
OH 26.4−1.9.....	July 7	1.93	2.15–2.32	360	HR 7236	B9 V	21000
	July 7	2.02	2.27–2.44	160			
	July 7	1.57	2.88–3.22	216			
	July 7	1.78	3.16–3.50	86			
	July 7	2.20	3.44–3.78	76			
	July 8	1.28	2.15–2.32	180	HR 7063	G4 Ia	4500
	July 8	1.25	2.27–2.44	80			
	July 8	1.21	2.88–3.22	27			
	July 8	1.13	3.16–3.50	7.2			
	July 8	1.12	3.44–3.78	6.3			
OH 26.5+0.6.....	July 6	1.15	2.15–2.32	180	HR 7236	B9 V	21000
	July 6	1.10	2.27–2.44	405			
	July 6	1.10	2.88–3.22	7.2			
	July 6	1.12	3.16–3.50	4.5			
	July 6	1.12	3.44–3.78	1.8			
OH 39.7+1.5.....	July 7	1.35	2.15–2.32	60	HR 7236	B9 V	21000
	July 7	1.37	2.27–2.44	40			
	July 7	1.41	2.88–3.22	9			
	July 7	1.32	3.16–3.50	5.4			
	July 7	1.25	3.44–3.78	1.8			
OH 44.8−2.2.....	July 7	1.30	2.15–2.32	8	HR 7235	A0 V	9600
	July 7	1.30	2.27–2.44	8			
	July 7	1.30	2.88–3.22	7.2			
	July 7	1.31	3.16–3.50	3.6			
	July 7	1.40	3.44–3.78	1.8			

that they be bright enough for us to observe on a telescope of modest aperture and obtain sufficient signal-to-noise ratio (S/N) to discern an H_2O ice absorption feature if there were one. The observations and data reduction are described in § 2, while the results and their implications for condensation in circumstellar envelopes are discussed in § 3.

2. OBSERVATIONS

The spectra of the OH/IR stars reported here were obtained at the Cerro Tololo Inter-American Observatory (CTIO) 1.5 m telescope on 1995 July 6–8 UT. The instrument used was the facility infrared spectrometer (IRS; see Depoy et al. 1990) equipped with a 256 × 256 InSb array. All observations were made with the 75 line mm^{-1} grating, which provided a 2 pixel spectral resolution of $\lambda/\Delta\lambda \sim 1320$ at 3.5 μm and $\sim$1650 at 2.2 μm. Spectra were obtained over the wavelength range 2.0–3.8 μm, which, at this resolution, required five different grating positions (2.15–2.32, 2.27–2.44, 2.88–3.22, 3.16–3.50, and 3.44–3.78 μm). The spatial resolution was 0.″95 $pixel^{-1}$. The 45″ long slit was kept at a width of $\sim$3″ for most of the observations because of the seeing conditions, except for a short time under excellent conditions on the night of July 7, when it was reduced to 2″ (the slit width has a significant effect on the 3 μm

TABLE 2

ADOPTED PARAMETERS FOR OH/IR STAR SAMPLE

Star	K (mag)	L (mag)	$\dot{M}_*$ (10^{-5} $M_\odot$ yr^{-1})	V_e (km s^{-1})	L_* ($L_\odot$)	τ_{ice}	N_{ice} (10^{16} cm^{-2})
OH 12.8−1.9	3.7	1.7	2.2	22.6	1.3×10^4	≤0.03	≤5.0
OH 20.3−0.1	6.3	3.0	3.1	16.5	1.4×10^4	≤0.03	≤5.0
OH 26.4−1.9	7.5	3.8	1.7	12.1	2.8×10^3	0.05	8.4
OH 26.5+0.6	7.6	1.5	0.9	14.1	1.5×10^4	0.23	34
OH 39.7+1.5	5.3	1.4	3.2	16.6	3.1×10^4	≤0.03	≤5.0
OH 44.8−2.3	5.5	2.0	2.4	15.9	4.1×10^4	≤0.03	≤5.0
OH 231.8+4.2.....	...	6.7	12	20	4.0×10^3	2.5	420
OH 32.8−0.3	...	3.6	18	16.4	1.1×10^4	0.7	120

NOTES.—Mass-loss rates from van der Veen 1989, Heske et al. 1990, Netzer & Knapp 1988, and Schutte & Tielens 1989; outflow velocities and luminosities from Herman & Habing 1985, Herman et al. 1986, Werner et al. 1980, and Sopka et al. 1985.

background). The long axis of the slit was oriented north-south. A log of the observations is given in Table 1.

The data were reduced using the IRAF image analysis software. Wavelength calibration was obtained by observing telluric emission lines (R. Elston 1996, private communication) and is estimated to be accurate to 15 Å. Atmospheric correction was achieved by dividing each spectrum by the spectrum of a standard star observed at a similar air mass (see Table 1). These stars were assumed to be adequately represented in this region of the spectrum by a blackbody. However, in some cases weak emission lines can be seen in the ratioed spectra of the OH/IR stars near 2.17, 3.04, 3.3, and 3.74 μm as a result of absorption by the Brγ, H I 10–5, H I 9–5, and Pfγ lines of atomic hydrogen in the standard stars. Flux calibration was achieved using the known K and L fluxes of the standard stars (see Table 2). It was necessary to multiply some of the spectral segments by a small correction factor to match the flux in the region that overlaps the longer wavelength segment. Flux differences like these result from seeing and/or small tracking and positioning errors. Between 2.5 and 2.9 μm the atmosphere is opaque, and the wavelength span of one grating setting is not large enough for there to be any overlap between these parts of the spectrum. Thus, the greatest *relative* flux uncertainty is between the 2.0–2.5 and 2.9–3.8 μm portions of the spectra. We estimate that this uncertainty may be as much as 20%. This uncertainty is still present even using the available K and L photometry for determining the short- and long-wavelength fluxes because of the potential variability of these stars.

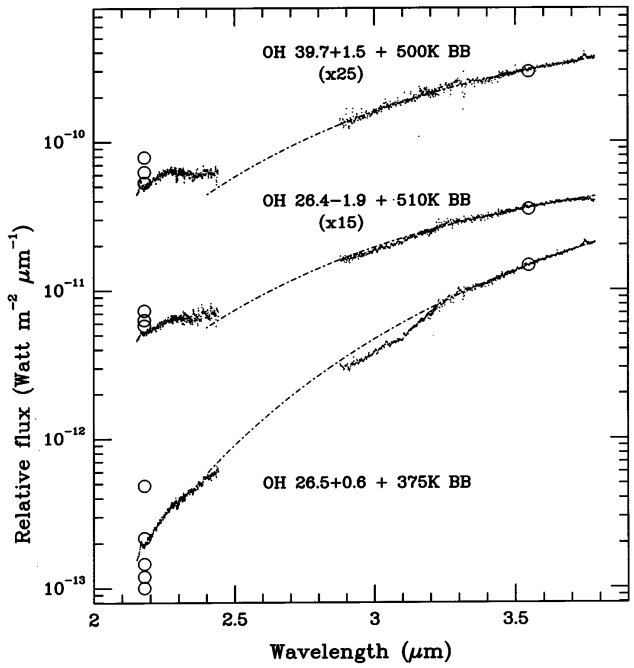

FIG. 1.—The 2–3.8 μm spectra of three of the OH/IR stars obtained at CTIO. The spectral resolution $\lambda/\Delta\lambda$ is $\sim$1650 at 2.2 μm and $\sim$1320 at 3.45 μm. Spectra obtained of OH 12.8−1.9, OH 20.3−0.1, and OH 44.8−2.3 are qualitatively similar to the OH 39.7 spectrum shown. The dot-dashed lines show our best estimate of the continuum. Circles are representative published KL photometry, scaled to match the observed spectral flux at the corresponding wavelength in the L band. The intrinsic variability of the central stars produces much of the KL color range (Engels et al. 1983). Photometry from Allen et al. (1977), Engels et al. (1983), Fix & Mutel (1984), Gosnell, Hudson, & Puetter (1979), Grasdalen (1983), Nyman, Hall, & Le Bertre (1993), Werner et al. (1980), and Willems & de Jong (1982).

3. RESULTS AND DISCUSSION

3.1. *Results*

The spectra of three of the six observed OH/IR stars are presented in Figure 1. Inspection of Figure 1 reveals clear H_2O ice absorption in the spectrum of OH 26.5+0.6 and probably also in OH 26.4−1.9. For the sake of clarity, only the spectrum obtained for one of the other four observed OH/IR stars, OH 39.7+1.5, is included in Figure 1 as a representative example. There is little, if any, evidence for ice in the lines of sight to these latter four objects. However, as an objective measure of the amount of H_2O ice absorption present, we have calculated the strength of the absorption at 3.1 μm in each source. These data are listed in Table 2. The uncertainty in any individual optical depth measurement, as shown, is on the order of $\pm$0.03; anything larger than this must be considered a possible detection of H_2O ice.

A determination of the optical depth requires fitting a continuum to each spectrum. While ideally we would take published stellar spectra, like those of Strecker, Erickson, & Witteborn (1979), and then redden them to fit the observed spectrum, in this case it is not that simple. In addition to a stellar continuum subject to substantial amounts of extinction, there is also clearly strong thermal emission from the dust envelopes around these stars (see Fig. 1). Therefore, in order to estimate an optical depth near 3.1 μm, we have elected to fit a simple blackbody to the spectral region between 2.9 and 3.8 μm, excluding the region containing the ice band (2.9–3.3 μm). Because of reddening and possible radiative transfer effects, the temperature of this blackbody is not particularly significant, so it is only used to conveniently define what appears to be an acceptable continuum. Without doing a full radiative transfer model for the star and envelope, this empirical approach seems to be the most straightforward way to obtain an estimate of the ice-band optical depth. The 3.1 μm optical depths calculated in this way are listed in Table 2.

We have also converted the 3.1 μm optical depth estimate to a column density of H_2O molecules in the solid state in the line of sight (this is only an upper limit on the column density if $\tau_{\rm ice} < 0.03$) using the formula

$$N(H_2O) = (\tau_{\rm ice}\,\Delta\nu/A)\,, \qquad (1)$$

where $\Delta\nu$ (cm^{-1}) is the FWHM optical depth and A (cm molecule^{-1}) is the integrated absorption intensity (d'Hendecourt & Allamandola 1986). Table 2 lists these column densities. It is important to note that in this calculation we used the data for 10 K H_2O ice, which may be lower than the actual ice temperature. In the absence of a high-S/N observed ice-band profile, it is difficult to estimate an ice temperature, but on the basis of the ice bands observed in other circumstellar envelopes and models of the condensation in the outflows of red giants, a nominal temperature of 80–110 K seems more reasonable (e.g., Smith et al. 1988; Jura & Morris 1985). However, we do not have data (A, $\Delta\nu$) available for this temperature range, so there is some uncertainty in the column densities in Table 2, by at least a factor of 2, due to the changing strength and width of the ice band with temperature (Hagen, Tielens, & Greenberg 1981; Smith, Sellgren, & Tokunaga 1989). If the ice temperature is similar in all envelopes, this factor will be the same for all objects.

3.2. *Ice in OH 26.5+0.6*

Past observations of OH 26.5+0.6 by Forrest et al. (1978) appear to show a weak absorption feature near 3.1 μm. However, Forrest et al. dismissed the possibility that this could be due to H_2O ice because they believed that the grain temperature in the dense region of the circumstellar envelope was almost certainly greater than 100 K and that the ice would rapidly sublime above this temperature. Subsequent laboratory measurements have demonstrated that H_2O ice can survive under laboratory conditions up to 140–150 K before sublimation takes place (e.g., Hagen et al. 1981; Smith et al. 1994), and indeed, there have been several detections of H_2O ice in circumstellar envelopes subsequent to the measurements of Forrest et al. (see § 1).

Using a simple 375 K blackbody for a continuum, we have converted the OH 26.5+0.6 spectrum to an optical depth scale as described above, and plotted it in Figure 2. This figure clearly shows a 3.1 μm absorption feature in this object, with a peak optical depth of 0.23 ± 0.03. In an attempt to estimate the H_2O ice temperature from the absorption-feature profile, we have fitted a variety of different models to the OH 26.5+0.6 optical depth spectrum. These models, taken from Smith et al. (1989), are for H_2O ice–coated silicate spheres at a range of temperatures (23–100 K: see Smith et al. for details; note that only the 23 K model is shown in the figure). Unfortunately, the signal-to-noise ratio is too low to reliably estimate a temperature from modeling the ice-band profile, although the sharp turnover near 3.25 μm or absence of a long-wavelength "wing" is consistent with the appearance of the 3.1 μm feature in oxygen-rich envelopes (e.g., OH 231.8+4.2; Smith et al. 1988). In order to make it clear what is real structure in the OH 26.5+0.6 spectrum and what is simply scatter in the data points, in Figure 2 we have marked the positions of features resulting from H I absorption in the standard stars, as well as the positions of the strongest photospheric OH absorption features. Because OH 26.5+0.6 is a late-type star, we would expect to see photospheric OH lines in the spectrum of this and the other objects in our sample, with strengths increasing with spectral type (e.g., Smith, Sellgren, & Brooke 1993); however, the noise level in Figure 2 makes it difficult to discern individual lines.

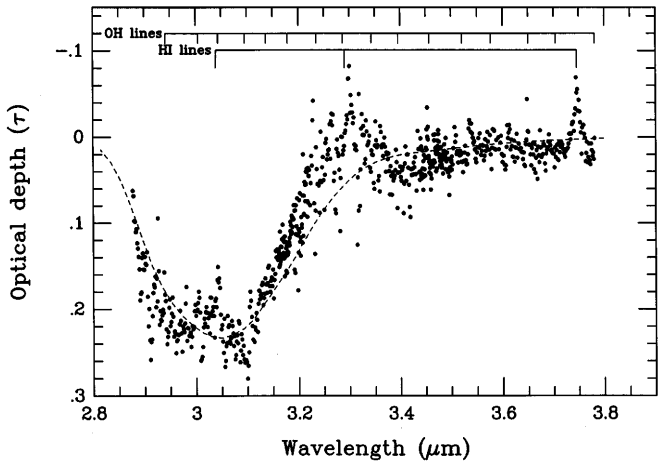

FIG. 2.—Spectrum of OH 26.5+0.6 between 2.8 and 3.8 μm, plotted on an optical depth scale. The dashed line is an example of the results of temperature models of H_2O ice–coated silicate grains (from Smith, Sellgren, & Tokunaga 1989). To clarify what is real structure and what is scatter in the data, the positions of the H I lines resulting from absorption in the standard star are marked. In addition, the positions of some of the stronger photospheric OH lines that could be present in the stellar spectrum are indicated.

3.3. *Discussion*

Given the apparent discrepancy between the unambiguous detection of strong H_2O ice bands in other OH/IR stars (e.g., OH 231.8+4.2; see § 1) and the absence of significant amounts of H_2O ice in most of the OH/IR stars in our sample, it is reasonable to ask whether any simple physical differences exist between our sample and those objects that do have ice.

Jura & Morris (1985) analyzed the conditions under which molecules condense onto preexisting grains in the outflows of mass-losing red giants. Their analytic solution for the ice-band optical depth, $\tau_{\rm ice}$, showed that it is predominantly a function of the luminosity of the star and the mass-loss rate of dust grains. In Table 2 we have included the observed 3.1 μm optical depths and column densities, along with the mass-loss rates, the outflow velocities, and the luminosities of our sample stars. The mass-loss rates are the most uncertain parameters in this table and are simple averages of estimates based on OH maser fluxes, *IRAS* 60 μm fluxes and 12-to-25 μm flux ratios of Heske et al. (1990) and the theoretical rates of Netzer & Knapp (1988), Schutte & Tielens (1989), and van der Veen (1989). In addition to our observed sample, we have also included data on the other two evolved stars in which H_2O ice absorption has already been detected and for which there are reliable mass-loss rates and luminosities.

Inspection of Table 2 suggests a correlation between the ice column density and the gas mass-loss rate. The ice column density is related to the column density of dust, which, in turn, depends on the dust mass-loss rate, $\dot{M}_{\rm gr}$. Although the exact form of the relationship between $\dot{M}_{\rm gr}$ and $\dot{M}_*$ is somewhat uncertain, because of the number of different ways in which mass-loss rates are measured (see, e.g., Heske et al. 1990), the dust-to-gas mass ratio in these objects is typically about 0.01 (Herman, Burger, & Pennix 1986). Hence, one might expect $\dot{M}_*$ to be a rough guide to those envelopes that contain ice, as shown in Figure 3*a*. Figure 3*b* shows that, ignoring those points that are just upper limits in Figure 3*b*, there appears to be a linear relationship between log $N_{\rm ice}$ and log $(\dot{M}_*/L_*)$. However, this is based on so few points that the relationship must be considered a tentative one at present.

It is worth looking for a theoretical basis for a correlation between log $N_{\rm ice}$ and log $(\dot{M}_*/L_*)$. The condensation of H_2O molecules at any radius r in the circumstellar envelope depends upon the balance of molecular accretion (i.e., sticking collisions) and desorption from the grains. The collision rate $\lambda(r)$ is $n_{\rm gr}\sigma_{\rm gr}V_D$, where $n_{\rm gr}$ is the grain number density, $\sigma_{\rm gr}$ is the grain geometric cross section, and V_D is the gas-grain drift speed (Jura & Morris 1985). Hence, $\lambda(r)$ scales with the circumstellar envelope parameters according to

$$\lambda(r) \propto \frac{r^{-2}\dot{M}_{\rm gr}V_D}{V_{\rm gr}} \propto \frac{r^{-2}\dot{M}_*V_D}{V_D+V_\infty} \propto \frac{r^{-2}\dot{M}_*}{1+(L_*Q_{\rm rp}V_\infty/\dot{M}_*c)^{1/2}}, \quad (2)$$

where $V_{\rm gr}$ is the grain speed, $Q_{\rm rp}$ is the flux-weighted mean of the dust radiation pressure efficiency, c is the speed of light, V_∞ is the terminal wind speed, and typically $V_\infty/V_D \approx 5$. In

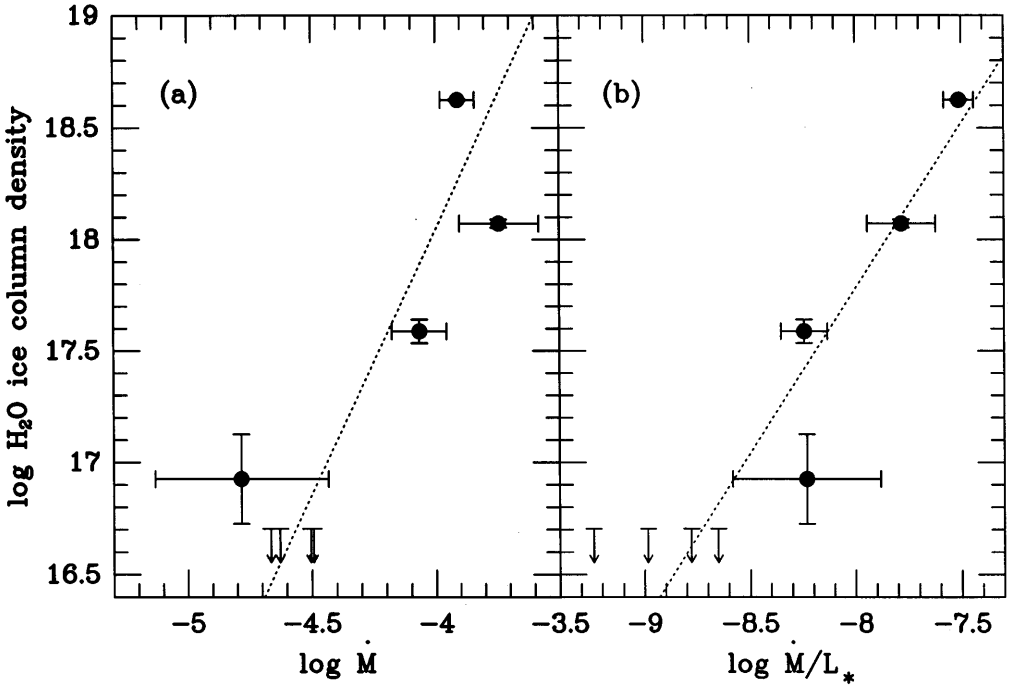

FIG. 3.—Plot of the measured H_2O ice column density (or upper limit to the column density) against (*a*) the mass-loss rate and (*b*) the ratio of the mass-loss rate to the luminosity. The dotted line is the best fit to those data points that have positive detections of H_2O ice. Data for these plots are shown in Table 2, and the sources of mass-loss rates and luminosities are indicated in the notes to this table and in the text.

the above relationships we have made use of the expression

$$V_D = \left(\frac{\dot{M}_* V_\infty c}{L_* Q_{\rm rp}}\right)^{1/2} \quad (3)$$

(Kwan & Hill 1977).

Hence, $\lambda(r)$ is a weak function of $\dot{M}_*/L_*$ but varies linearly with $\dot{M}_*$. The desorption rate of H_2O molecules from a grain at temperature $T_{\rm gr}$ is

$$\xi(r) = 10^{13} \exp\,(-6070/T_{\rm gr}) \quad (4)$$

(Jura & Morris 1985). For optically thin dust shells $T_{\rm gr} \propto (L_*/r^2)^{1/5}$, and so

$$\xi(r) \propto \exp\,(-Ar^2/L_*)^{1/5}\,, \quad (5)$$

where A is a constant. Thus we see that the $N_{\rm ice} \propto \dot{M}_*/L_*$ relationship can be justified qualitatively on physical grounds: high mass-loss rates increase the H_2O-grain collision rate, whereas low L_* yields lower dust temperatures and, so, longer surface retention times for accreted molecules.

Both OH 231.8+4.2 and IRAS 09371+1212 are known to be bipolar, and the ice absorption seen in the lines of sight toward them is believed to arise in circumstellar material. It is possible that the angle at which these objects are viewed might affect our measurement of the ice optical depth and thus distort the appearance of a relationship in Figure 3. However, to quantify the uncertainty introduced by this factor requires a knowledge of exactly where in the circumstellar material the ice condensation occurs and some judgment of whether the circumstellar material forms a disk, torus, or some other geometry. This sort of theoretical modeling is well beyond the scope of this paper. Because of this additional uncertainty, however, we emphasize that our suggestion of a possible relationship between $N_{\rm ice}$ and $\dot{M}_*/L_*$ needs to be investigated more fully by additional measurements before being accepted.

4. CONCLUSIONS

We have searched for water ice absorption in the envelopes of six OH/IR stars. We confirm the presence of ice in OH 26.5+0.6, report its tentative detection in OH 26.4−1.9, and present upper limits to the ice optical depths in the remainder of the sample.

Taken along with other published data, our results suggest a relationship between ice column density $N_{\rm ice}$ and the ratio $\dot{M}_*/L_*$. This relation may provide a crude but useful measure of the balance between sticking and retention of water molecules on dust grains in an envelope. However, a complete explanation of the $N_{\rm ice}$ variation in our sample may require a full radiative transfer treatment of the temperature variation in the circumstellar envelopes. $N_{\rm ice}$ is an integral quantity, and the actual temperature distribution plays a role in the amount of ice that can be condensed at any radius in the envelope. Most of the stars in our sample have optically thick envelopes. In this case, stellar photons are absorbed and reemitted deep in the envelope, leading to a radial temperature distribution that, compared with the optically thin case, yields higher temperatures close to the star and cooler ones farther out. This reduction in grain temperature in regions where the gas-grain collision rate is high produces conditions that are more conducive for ice to condense. Unfortunately, without more observations of ice column densities near the detection limit, we cannot determine whether the apparent $N_{\rm ice} \propto \dot{M}_*/L_*$ relation holds up for lower values of $\dot{M}_*/L_*$, nor can we estimate a minimum mass-loss rate and luminosity for H_2O ice condensation, or the values for which a catastrophic freeze-out of the gas-phase water molecules might occur. It would be an interesting test to measure $N_{\rm ice}$

in other OH/IR stars whose $\dot{M}_*/L_*$ ratios fall in the same region of the plot. For example, one object for which we would predict a very large ice column density is OH 17.7−2.0.

We thank the staff of CTIO for their hospitality and support and particularly R. Elston for his assistance at the telescope. An anonymous referee provided several useful suggestions that improved the paper. The work of S. B. C. was supported by NASA's Origins of Solar Systems Program. Funds for this study have been allocated by NASA Ames under Interchange NCC 2-1592. Y. J. P. is supported by NASA's Exobiology Program, 344-38-12-09.

REFERENCES

Allen, D. A., Hyland, A. R., Longmore, A. J., Caswell, J. L., Goss, W. M., & Haynes, R. F. 1977, ApJ, 217, 108
Charnley, S. B., & Smith, R. G. 1993, in IAU Symp. 155, Planetary Nebulae, ed. R. Weinberger & A. Acker (Dordrecht: Kluwer), 329
DePoy, D. L., Gregory, B., Elias, J., Montané, A., Pérez, G., & Smith, R. M. 1990, PASP, 120, 1433
d'Hendecourt, L. B., & Allamandola, L. J. 1986, A&AS, 64, 453
Eiroa, C., Hefele, H., & Qian, Z.-Y. 1983, A&AS, 54, 309
Engels, D., Kreysa, E., Schultz, G. V., & Sherwood, W. A. 1983, A&A, 124, 123
Fix, J. D., & Mutel, R. L. 1984, AJ, 89, 406
Forrest, W. J., et al. 1978, ApJ, 219, 114
Geballe, T. R., Kim, Y. H., Knacke, R. F., & Noll, K. S. 1988, ApJ, 326, L65
Gillett, F. C., & Soifer, B. T. 1976, ApJ, 207, 780
Gosnell, T. R., Hudson, H., & Puetter, R. C. 1979, AJ, 84, 538
Grasdalen, G. 1983, ApJS, 53, 413
Hagen, W., Tielens, A. G. G. M., & Greenberg, J. M. 1981, Chem. Phys., 56, 367
Herman, J., Burger, J. H., & Pennix, W. H. 1986, A&A, 167, 247
Herman, J., & Habing, H. J. 1985, A&AS, 59, 523
Heske, A., Forveille, T., Omont, A., van der Veen, W. E. C. J., & Habing, H. J. 1990, A&A, 239, 173
Hodapp, K. W., Sellgren, K., & Nagata, T. 1988, ApJ, 326, L61
Jones, T. J., Hyland, A. R., & Gatley, I. 1983, ApJ, 273, 660
Jura, M., & Morris, M. 1985, ApJ, 292, 487
Kwan, J., & Hill, F. 1977, ApJ, 215, 781
Nakagawa, N. 1980, in IAU Symp. 87, Interstellar Molecules, ed B. H. Andrew (Dordrecht: Reidel), 365
Netzer, N., & Knapp, G. R. 1988, ApJ, 323, 734
Nyman, L.-Å., Hall, P. J., & Le Bertre, T. 1993, A&A, 280, 551
Roche, P. F., & Aitken, D. K. 1984, MNRAS, 209, 33P
Rouan, D., Omont, A., Lacombe, F., & Forveille, T. 1988, A&A, 189, L3
Schutte, W. A., & Tielens, A. G. G. M. 1989, ApJ, 343, 369
Smith, R. G., Robinson, G., Hyland, A. R., & Carpenter, G. L. 1994, MNRAS, 271, 481
Smith, R. G., Sellgren, K., & Brooke, T. Y. 1993, MNRAS, 263, 749
Smith, R. G., Sellgren, K., & Tokunaga, A. T. 1988, ApJ, 334, 209
———. 1989, ApJ, 344, 413
Sopka, R. J., Hildebrand, R., Jaffe, D. T., Gatley, I., Roellig, T., Werner, M., Jura, M., & Zuckerman, B. 1985, ApJ, 294, 242
Strecker, D. W., Erickson, E. F., & Witteborn, F. C. 1979, ApJS, 41, 501
Tielens, A. G. G. M. 1983, ApJ, 271, 702
van der Veen, W. E. C. J. 1988, Ph.D. thesis, Leiden Univ.
———. 1989, A&A, 210, 127
Werner, M. W., Beckwith, S., Gatley, I., Sellgren, K., Berriman, G., & Whiting, D. L. 1980, ApJ, 239, 540
Willems, L., & de Jong, T. 1982, A&A, 115, 213